Deep Learning Based Person Authentication Hand Radiographs

^[1]E.DilipKumar, R.Praveen Kumar

^{[1][2]} Department of MCA, Dhanalakshmi Srinivasan college of engineering and Technology

^[1] mailtodilip82@gmail.com,^[2] praveenkumarr.mca2021@dscet.ac.in

Abstract: Authentication is the process of automatically recognizing the correct person. Presently, the biometric identification systems are based on static features like face[2], iris[3], palm print[4], voice[5] and fingerprint impression of the user, which mostly remains unchanged over time. The performance of a biometric identification system is measured based on accuracy, efficiency, security, and privacy. Biometric systems are a combination of multiple sensors, multiple algorithms, and numerous instances, making it more accurate, reliable, secure, and robust[6]. Identifying an injured person is challenging in disasters like tsunamis and earthquakes and catastrophic accidents. In such cases hand radiographs may be considered. Because bones cannot be easily damaged. The existing method uses KNN (K-Nearest Neighbor) classifier[8]. It consists of training and testing stage. In training stage, CNN is applied which includes mainly convolution layer, ReLU layer and Max pooling layer. The proposed method uses CNN classifier. It consists of training and testing stage.

1. INTRODUCTION

CNN is applied which includes mainly convolution layer, ReLU layer and Max pooling layer. In the proposed work Person Authentication is performed with the hand radiographs using Image processing and deep learning concept[1]t. Three-layered convolutional deep-learning architecture is used for the pre-processing, feature extraction and max pooling layer. An individual's identity is ascertained using these three layers[7].

CNN is inspired by the biological phenomenon of the animal visual cortex, which shows the connectivity pattern between different neurons. CNN has a wide range of applications such as image processing, video processing, speech processing, and natural language processing. CNN consists of four significant steps, such as convolution layer, rectified linear unit (ReLU), maximum pooling layer, and fully connected layer.

In the convolution layer, an image is multiplied by filter kernel, which may have some negative values. These negative values bring the non-linearity in the image. The non-linearity is then removed by using the rectified linear unit layer by converting all the negative values to zero usingwhere, IReLU is the ReLU layer image and Iconv is the convolutional layer image. The ReLU layer output size is 200X200X3, which is equal to the size of the convolution layer output. The output of the ReLU layer is given to max pooling layer.

Pooling is used for the minimization of the computing cost by reducing the dimension of the ReLU layer output. Pooling is also used to retain the position and rotational invariant features of an image. There are two types of pooling methods: Maximum and Average pooling. In maximum pooling, the maximum value of the given window is selected, while in average pooling, the average value of the window is selected . Unlike average pooling, maximum pooling suppresses the noise in the image along with feature reduction. Pooling is also used to maintain the localization of the shape of the local object in the image. The window size of 2×2 is selected for maximum pooling, which reduced the size to exactly half of the ReLU layer ($100\times75\times6$). The larger window size for the maximum pooling may result in the fine local information of the image.

A binary image is a digital image that has only two possible values for each pixel. Typically the two colors used for a binary image are black and white though any two colors can be used. The color used for the object(s) in the image is the foreground color while the rest of the image is the background color. Binary images are also called bi-level or two-level. This means that each pixel is stored as a single bit (0 or 1)

A gray scale Image is digital image is an image in which the value of each pixel is a single sample, that is, it carries only intensity information. Images of this sort, also known as black-and-white, are composed exclusively of shades of gray (0-255), varying from black (0) at the weakest intensity to white (255) at the strongest. Gray scale images are distinct from one-bit black-and-white images, which in the context of computer imaging are images with only the two colors, black, and white (also called bi-level or binary images). Gray scale images have many shades of gray in between. Gray scale images are also called on monochromatic, denoting the absence of any chromatic variation. Gray scale images are often the result of measuring the intensity of light at each pixel in a single band of the electromagnetic spectrum (e.g. infrared, visible light, ultraviolet, etc.), and in such cases they are monochromatic proper when only a



Vol. 8, Issue 6, June 2023

given frequency is captured. But also they can be synthesized from a full color image.

Authentication is the process of automatically recognizing the correct person. Presently, the biometric identification systems are based on static features like face[2], iris[3], palm print[4], voice[5] and fingerprint impression of the user, which mostly remains unchanged over time. The performance of a biometric identification system is measured based on accuracy, efficiency, security, and privacy. Biometric systems are a combination of multiple sensors, multiple algorithms, and numerous instances, making it more accurate, reliable, secure, and robust[6]. Identifying an injured person is challenging in disasters like tsunamis and earthquakes and catastrophic accidents. In such cases hand radiographs may be considered. Because bones cannot be easily damaged.

The existing method uses KNN (K-Nearest Neighbor) classifier[8]. It consists of training and testing stage. In training stage, CNN is applied which includes mainly convolution layer, ReLU layer and Max pooling layer. The proposed method uses CNN classifier. It consists of trainingand testing stage.

PROJECT DESCRIPTION:

This project 'Deep learning based Person Authentication using Hand Radiographs' is essentially a pattern recognition system that makes use of biometric traits to recognize individuals. The texture of the hand radiographs of different individuals has been proven to be distinctive even among identical twins.

OBJECTIVES OF THE PROJECT:

The objective of the project is to Authenticate a Person using Deep Learning. Deep-learning architecture has three layers, they are processing, feature extraction and max pooling layer. An individual's identity is ascertained using these three layers. **SYSTEM ANALYSIS**

INTRODUCTION:

Design is the first step in the development phase for any techniques and principles for the purpose of defining a device, a process or system in sufficient detail to permit its physical realization. Once the software requirement have been analyzed and specified the software design involving three technical activities-design, coding, implementation and testing that are required to build and verify the software.

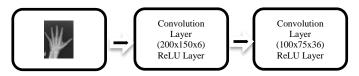
SYSTEM STUDY:

The specific details of the project are specified by the person authentication using hand radiographs. In this document, various steps involved in the existing system process have been explained. In the project have the used to base on hand radiographs using a deep learning. Three-layered convolutional deep-learning architecture is used for the pre-processing, feature extraction and max pooling layer. An individual's identity is ascertained using these three layers.

EXISTING SYSTEM:

The logical module of the existing method using KNN classifier. It consists of training and testing stage. In training stage, CNN is applied which includes mainly convolution layer, ReLU layer and Max pooling layer.

The existing method using three CNN layers. The first CNN layer resize the image to 200x150 and then passes it to ReLU layer. The 6x6 matrix is used ReLU layer (200x150x6). The max pooling layer subtracts the maximum value from the ReLU layer and converts the image to 100x75x6. The second CNN layer resize the image to 100x75x36 and then passes it to ReLU layer. The 6x6 matrix is used ReLU layer (100x75x36). The max pooling layer subtracts the maximum value from the ReLU layer and converts the image to 50x37x36. The last CNN layer resize the image to 50x37x216 and then passes it to ReLU layer. The 6x6 matrix is used ReLU layer (50x37x216). The max pooling layer subtracts the maximum value from the ReLU layer. The 6x6 matrix is used ReLU layer (50x37x216). The max pooling layer subtracts the maximum value from the ReLU layer. The 6x6 matrix is used ReLU layer (50x37x216). The max pooling layer subtracts the maximum value from the ReLU layer. The 6x6 matrix is used ReLU layer (50x37x216). The max pooling layer subtracts the maximum value from the ReLU layer and converts the image to 25x18x216. Finally the hand radiograph image is converted to 97200x1 in the fully connected layer. The image derived from the fully connected layer is used in the KNN classifier. Finally the identity of the individual is authenticated or unauthenticated is shown in figure 2.3.





Vol. 8, Issue 6, June 2023

PROPOSED SYSTEM:

The logical module of the proposed method using CNN classifier. It consists of training and testing stage. CNN is applied which includes mainly convolution layer, ReLU layer and Max pooling layer.

The proposed method using five CNN layers. The first CNN layer resize the image to 200x200 and then passes it to ReLU layer. The 3x3 matrix is used ReLU layer (200x200x3). The max pooling layer subtracts the maximum value from the ReLU layer and converts the image to 100x100x3. The second CNN layer resize the image to 100x100x9 and then passes it to ReLU layer. The 3x3 matrix is used ReLU layer (100x100x9). The max pooling layer subtracts the maximum value from the ReLU layer and converts the image to 50x50x9. The third CNN layer resize the image to 50x50x27 and then passes it to ReLU layer. The 3x3 matrix is used ReLU layer (50x50x27). The max pooling layer subtracts the maximum value from the ReLU layer and converts the image to 25x25x27. The fourth CNN layer resize the image to 25x25x81 and then passes it to ReLU layer. The 3x3 matrix is used ReLU layer (25x25x81). The max pooling layer subtracts the maximum value from the ReLU layer and converts the image to 13x13x81. The last CNN layer resize the image to 25x25x243 and then passes it to ReLU layer. The 6x6 matrix is used ReLU layer (25x25x243). The max pooling layer subtracts the maximum value from the ReLU layer and converts the image to 13x13x243.

Finally the hand radiograph image is converted to 41067x1 in the fully connected layer. The image derived from the fully connected layer is used in the CNN classifier. Finally the identity of the individual is authenticated or unauthenticated is shown in

2.5 MODULE DESCRIPTION:

The project includes five processing modules, they are:

- 1. Loading of data set
- 2. Pre-Processing
- 3. Feature extraction
- 4. Trained and test data
- 5. Output

2.5.1 LOADING OF DATA SET

The input data set is downloaded from the kaggle website. The downloaded data set includes four thousand sixty four rows and four columns. From this only seventy hand radiograph data sets were extracted.

2.5.2 PRE-PROCESSING

Pre-processing is an improvement of the image data that suppresses unwilling distortions or enhances some image features important for further processing, although geometric transformations of images like resize, hand segmentation, background removal, rotation and normalization are classified among pre-processing methods. This project uses resize and normalization process method.

2.5.3 FEATURE EXTRACTION

Feature extraction refers to the process of transforming raw data into numerical features that can be processed while preserving the information in the original data set. It yields better results than applying machine learning directly to the raw data. ReLU Layer and Maxpooling layer is used in feature extraction module.

2.5.4 TRAINED AND TEST DATA

Train/Test is a method to measure the accuracy of your model. It is called Train/Test because you split the data set into two sets: a training set and a testing set. Example 80% for training and 20% for testing.

2.5.5 **OUTPUT**

The hand radiograph image in the output module is available in two format. One is authorized person and another one is unauthorized person. Authorized person has 30 images and unauthorized person has 40 images.

2.6 CONCLUSION

This chapter outlines the total system analysis performed with respect to user system specification, System Study based project specification Requirement Analysis, and the Modules Proposed. Further in the next chapter, the system design and development are addressed.

SYSTEM DESIGN AND DEVELOPMENT

3.1 INTRODUCTION

The system analysis follows system design with two major aspects namely, i) Logical design and ii) physical design. Following the design, the development of the system based on coding design using the chosen software technologies is carried out.

3.2 LOGICAL DESIGN

The logic design of the system is conceived and represented using some standard design elements such as algorithmic procedures, Block Diagram, Sequence Diagram and etc.

3.2.1 BLOCK DIAGRAM

A Block diagram is a static structural diagram that shows system components, their contents and interfaces and relationships.



International Journal of Innovative Research in Management, Engineering, and Technology Vol. 8, Issue 6, June 2023

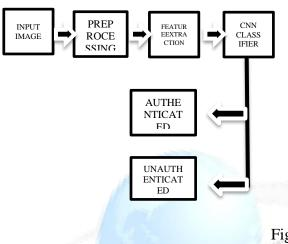


Figure 3.2.1 Block Diagram

The above diagram illustrates the modules relationship in the project is shown in figure 3.2.1. 3.3 PHYSICAL DESIGN

The physical design contains the dataset design (tables & images).

3.4 DATA SET

The data set is downloaded from the kaggle website (http://www.kaggle.com).

The downloaded data set includes four thousand sixty four rows and four columns. From this only seventy hand radiograph data sets were extracted. Because they are all PNG (Portable Network Graphics) file. The PNG File format is widely used on website to display high-quality digital image. A PNG File is used by many editing programs and software is shown in table 3.4. Table 3.4: Data set image format table

| S. NO. | IMAGE | TYPE | SIZE |
|--------|--------|----------|----------|
| | NUMBER | | |
| 1 | 4360 | PNG File | 302 KB |
| 2 | 4361 | PNG File | 395 KB |
| 3 | 4362 | PNG File | 2,813 KB |
| 4 | 4363 | PNG File | 316 KB |
| 5 | 4364 | PNG File | 266 KB |
| 6 | 4365 | PNG File | 327 KB |
| 7 | 4366 | PNG File | 282 KB |
| 8 | 4367 | PNG File | 248 KB |
| 9 | 4368 | PNG File | 372 KB |
| 10 | 4369 | PNG File | 2,073 KB |
| 11 | 4370 | PNG File | 422 KB |
| 12 | 4371 | PNG File | 1,192 KB |
| 13 | 4372 | PNG File | 338 KB |
| 14 | 4373 | PNG File | 242 KB |
| 15 | 4374 | PNG File | 303 KB |
| 16 | 4375 | PNG File | 254 KB |
| 17 | 4376 | PNG File | 342 KB |
| 18 | 4377 | PNG File | 1,271 KB |
| 19 | 4378 | PNG File | 286 KB |



| Internati | | Vol. 8, Issu | e 6, June 2023 | and rec | Jinology |
|-----------|----|--------------|----------------|----------|----------|
| | | | | | |
| | | | | | |
| | 20 | 4379 | PNG File | 3,258 KB | _ |
| | 21 | 4380 | PNG File | 1,295 KB | _ |
| | 22 | 4381 | PNG File | 926 KB | _ |
| | 23 | 4382 | PNG File | 193 KB | _ |
| | 24 | 4383 | PNG File | 322 KB | _ |
| | 25 | 4384 | PNG File | 778 KB | _ |
| | 26 | 4385 | PNG File | 226 KB | _ |
| | 27 | 4386 | PNG File | 215 KB | _ |
| | 28 | 4387 | PNG File | 299 KB | _ |
| | 29 | 4388 | PNG File | 1,155 KB | _ |
| | 30 | 4389 | PNG File | 169 KB | _ |
| | 31 | 4520 | PNG File | 3,196 KB | _ |
| | 32 | 4521 | PNG File | 1,313 KB | _ |
| | 33 | 4522 | PNG File | 2,132 KB | _ |
| | 34 | 4523 | PNG File | 1,691 KB | _ |
| | 35 | 4524 | PNG File | 1,259 KB | _ |
| | 36 | 4525 | PNG File | 1,199 KB | _ |
| | 37 | 4526 | PNG File | 1,031 KB | _ |
| | 38 | 4527 | PNG File | 304 KB | _ |
| | 39 | 4528 | PNG File | 1,764 KB | _ |
| | 40 | 4529 | PNG File | 355 KB | _ |
| | 41 | 4530 | PNG File | 2,349 KB | _ |
| | 42 | 4531 | PNG File | 1,127 KB | _ |
| | 43 | 4532 | PNG File | 277 KB | _ |
| | 44 | 4533 | PNG File | 1,649 KB | _ |
| | 45 | 4534 | PNG File | 876 KB | _ |
| | 46 | 4535 | PNG File | 182 KB | _ |
| | 47 | 4536 | PNG File | 1,080 KB | _ |
| | 48 | 4537 | PNG File | 320 KB | _ |
| | 49 | 4538 | PNG File | 1,330 KB | _ |
| | 50 | 4539 | PNG File | 1,325 KB | _ |
| | 51 | 4540 | PNG File | 3,454 KB | _ |
| | 52 | 4541 | PNG File | 3,639 KB | _ |
| | 53 | 4542 | PNG File | 1,763 KB | _ |
| | 54 | 4543 | PNG File | 1,066 KB | _ |
| | 55 | 4544 | PNG File | 175 KB | _ |
| | 56 | 4545 | PNG File | 294 KB | _ |
| | 57 | 4546 | PNG File | 254 KB | 4 |
| | 58 | 4547 | PNG File | 570 KB | 4 |
| | 59 | 4548 | PNG File | 288 KB | 4 |
| | 60 | 4549 | PNG File | 3,308 KB | 4 |
| | 61 | 4550 | PNG File | 3,474 KB | 4 |
| | 62 | 4551 | PNG File | 3,375 KB | |



ISSN (Online): 2456-0448

International Journal of Innovative Research in Management, Engineering, and Technology

| | Vol. 8, Issu | | |
|----|--------------|----------|----------|
| | | | |
| 63 | 4552 | PNG File | 1,107 KB |
| 64 | 4553 | PNG File | 170 KB |
| 65 | 4554 | PNG File | 196 KB |
| 66 | 4555 | PNG File | 1,224 KB |
| 67 | 4556 | PNG File | 239 KB |
| 68 | 4557 | PNG File | 244 KB |
| 69 | 4558 | PNG File | 227 KB |
| 70 | 4559 | PNG File | 291 KB |

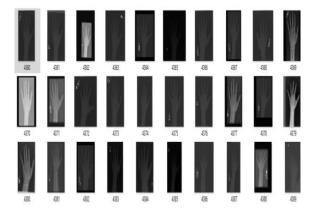


Figure 3.4 Sample images of hand radiographs from the dataset **3.5 MODULES:**

The project includes five processing modules, they are:

- 1. Loading of data set
- 2. Pre-Processing
- 3. Feature extraction
- 4. Trained and test data
- 5. Output

3.5.1 LOADING OF DATA SET

The input data set is downloaded from the kaggle website. The downloaded data set includes four thousand sixty four rows and four columns. From this only seventy hand radiograph data sets were extracted. Because they are all PNG (Portable Network Graphics) file. The PNG File format is widely used on website to display high-quality digital image is shown in figure 3.5.1.1, 3.5.1.2 and 3.5.1.3.



Vol. 8, Issue 6, June 2023

| Name | Size | Packed | Туре | Modified | CRC32 |
|----------------|------|--------|------------------|----------------|----------|
| VOC2007_28.mat | 569 | 543 | Microsoft Access | 14-07-20 07:13 | C13D0F73 |
| VOC2007_27.mat | 339 | 295 | Microsoft Access | 14-07-20 07:13 | 14A67BF0 |
| VOC2007_26.mat | 421 | 383 | Microsoft Access | 14-07-20 07:13 | 57C7A3E1 |
| VOC2007_25.mat | 339 | 295 | Microsoft Access | 14-07-20 07:13 | EE2C73E8 |
| VOC2007_24.mat | 419 | 382 | Microsoft Access | 14-07-20 07:13 | C0730D95 |
| VOC2007_23.mat | 421 | 384 | Microsoft Access | 14-07-20 07:13 | C0BD1247 |
| VOC2007_22.mat | 571 | 544 | Microsoft Access | 14-07-20 07:13 | 2EB41FB4 |
| VOC2007_21.mat | 492 | 457 | Microsoft Access | 14-07-20 07:13 | 34235753 |
| VOC2007_20.mat | 423 | 386 | Microsoft Access | 14-07-20 07:13 | ABEA1344 |
| VOC2007_19.mat | 422 | 385 | Microsoft Access | 14-07-20 07:13 | 6983ECF4 |
| VOC2007_18.mat | 337 | 294 | Microsoft Access | 14-07-20 07:13 | DEF045DA |
| VOC2007_17.mat | 421 | 383 | Microsoft Access | 14-07-20 07:13 | 40EDD917 |
| VOC2007_16.mat | 338 | 294 | Microsoft Access | 14-07-20 07:13 | F9C3976B |
| VOC2007_15.mat | 495 | 463 | Microsoft Access | 14-07-20 07:13 | 53FDA1DE |
| VOC2007_14.mat | 780 | 768 | Microsoft Access | 14-07-20 07:13 | 4E606324 |
| VOC2007_13.mat | 338 | 295 | Microsoft Access | 14-07-20 07:13 | 1C051B0E |
| VOC2007_12.mat | 420 | 383 | Microsoft Access | 14-07-20 07:13 | 417F2306 |
| VOC2007_11.mat | 421 | 384 | Microsoft Access | 14-07-20 07:13 | 44DE2BC0 |
| VOC2007_10.mat | 421 | 383 | Microsoft Access | 14-07-20 07:13 | AB4EB25B |
| VOC2007_9.mat | 497 | 464 | Microsoft Access | 14-07-20 07:13 | 6FBD6C4E |
| VOC2007_8.mat | 573 | 547 | Microsoft Access | 14-07-20 07:13 | 8682B263 |
| VOC2007_7.mat | 339 | 296 | Microsoft Access | 14-07-20 07:13 | 9D5E9D7F |
| VOC2007_6.mat | 494 | 459 | Microsoft Access | 14-07-20 07:13 | 47E8AD21 |
| VOC2007_5.mat | 339 | 296 | Microsoft Access | 14-07-20 07:13 | 5EB72860 |
| VOC2007_4.mat | 489 | 455 | Microsoft Access | 14-07-20 07:13 | FB99D8D2 |
| VOC2007_3.mat | 497 | 465 | Microsoft Access | 14-07-20 07:13 | BD7D8C78 |
| VOC2007_2.mat | 336 | 293 | Microsoft Access | 14-07-20 07:13 | 1E9DD893 |
| VOC2007_1.mat | 420 | 382 | Microsoft Access | 14-07-20 07:13 | 01EB90CE |

Figure 3.5.1.1 Downloaded dataset from kaggle website

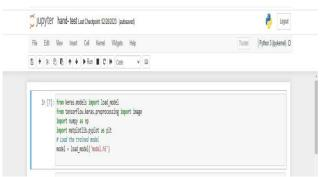


Figure 3.5.1.2 Code for loading of data set

| total_sa | <pre>mple = train_generator.n</pre> | |
|----------|---|--|
| n_epochs | : = 30 | |
| | <pre>= model.fit_generator(train_generator, steps_per_epoch-int(total_sample/batch_size), epochsn.goochs, verbose=1)</pre> | |
| model.sa | <pre>ive('model.h5')</pre> | |

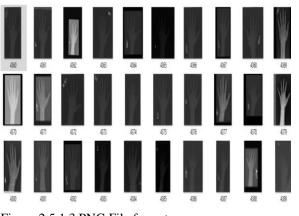


Figure 2.5.1.3 PNG File format

3.5.2 PRE-PROCESSING

Pre-processing is an improvement of the image data that suppresses unwilling distortions or enhances some image features important for further processing, although geometric transformations of images like resize, hand segmentation, background removal, rotation and normalization are classified among pre-processing methods.

In the preprocessing method, the Kera's library is imported from the tensor flow software. A convolutional 2D layer is imported from an imported Kera's library. Then the numpy library is imported. The numpy is used to convert the downloaded image into an array. This project uses resize and normalization process method. The hand radiographs image is resizes into 200x200 as shown in figure 3.5.2. This is because all hand radiographs images should be the same size. A hand radiograph image can be processed in ReLU and maxpooling layers only if they are of the same size.



Figure 3.5.2 Code for working of CNN algorithm



Vol. 8, Issue 6, June 2023

3.5.3 FEATURE EXTRACTION

Feature extraction refers to the process of transforming raw data into numerical features that can be processed while preserving the information in the original data set. It yields better results than applying machine learning directly to the raw data.

ReLU Layer and Maxpooling layer is used in feature extraction module. Maxpooling layer is imported from Kera's library. There are five types feature extraction methods for hand radiograph image. They are radius-ulna, carpal, metacarpal, phalanges and epiphysis. The ReLU (Rectified Linear Unit) is not a separate component of the convolutional neural network process. The ReLU layer is to improve the nonlinearity of the image's pixel data. Maxpooling returns the maximum value from the portion of the image covered by the kernel.

3.5.4 TRAINED AND TEST DATA

Train/Test is a method to measure the accuracy of your model. It is called Train/Test because the splitted data set is into two sets: a training set and a testing set. Example 80% for training and 20% for testing.

Epoch= total sample / batch size

In the training stage a hand radiographs image is divided into 30 epochs. Each epoch is trained separately based on above formula is shown in figure 3.5.4.1. Each epoch to gives accuracy and loss and it is shown in figure 3.5.4.2. The graph is drawn to predict the accuracy and loss of calculated epoch. Accuracy and loss is drawn based on epoch versus time duration. Accuracy graph interpreted it is positively correlated which implied if epoch increases with duration. Loss graph interpreted it is negatively correlated which stands the epoch decreases while duration increases is shown in figure 3.5.4.3.

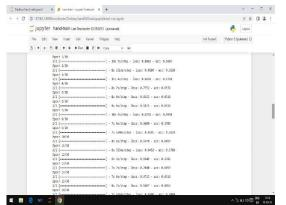


Figure 3.5.4.2 Code for training epoch



Figure 3.5.4.3 Graph for Training Accuracy and Training Loss



A hand radiograph image path is copied during the test stage. Converts the copied image to 200x200. The transformed image is converted to array and then the hand radiograph image is sent to the output module for better quality is shown in figure 3.5.4.4.

```
Copyright to IJIRMET
```



Figure 3.5.4.4 Code for testing data

3.5.5 OUTPUT

The hand radiograph image in the output module is available in two format. One is authorized person and another one is unauthorized person. Authorized person has 30 images and unauthorized person has 40 images is shown in figure 3.5.5.1 and 3.5.5.2.



Figure 3.5.5.1 Output of Authorized person

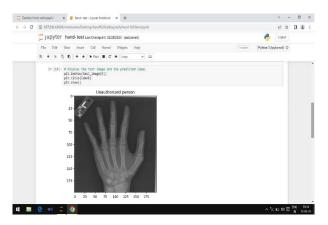


Figure 3.5.5.2 Output for Unauthorized person

4.2 SYSTEM IMPLEMENTATION

In the project have the used to base on hand radiographs using a deep learning. Three-layered convolutional deep-learning architecture is used for the pre-processing, feature extraction and max pooling layer. An individual's identity is ascertained using these three layers. **4.2.1 CONVOLUTION NEURAL NETWORK**

CNN is inspired by the biological phenomenon of the animal visual cortex, which shows the connectivity pattern between different neurons. CNN has a wide range of applications such as image processing, video processing, speech processing, and natural language processing. CNN consists of four significant steps, such as convolution layer, rectified linear unit (ReLU), maximum pooling layer, and fully connected layer. The architecture of the CNN single layer is shown in Fig.4.2.1.

The hand radiograph image obtained in this project is used five convolution layer. The hand radiograph image is converted to first layer 200x200x3, the second layer 100x100x9, third layer 50x50x27, fourth layer 25x25x81 and finally 25x25x243. The hand radiograph image is more accurate enhances by using five convolution layer.

Copyright to IJIRMET





Figure 4.2.1 The architecture of the CNN Layer

4.2.2 ReLU LAYER

In the convolution layer, an image is multiplied by filter kernel, which may have some negative values. These negative values bring the non-linearity in the image. The non-linearity is then removed by using the rectified linear unit layer by converting all the negative values to zero usingwhere, IReLU is the ReLU layer image and Iconv is the convolutional layer image. The ReLU layer output size is 200X200X3, which is equal to the size of the convolution layer output. The output of the ReLU layer is given to max pooling layer . The hand radiograph image obtained in this project is used five ReLU layer. The hand radiograph image is converted to first layer 200x200x3, the second layer 100x100x9, third layer 50x50x27, fourth layer 25x25x81 and finally 25x25x243. The hand radiograph image is more accurate enhances by using five ReLU layer.

4.2.3 MAX POOLING LAYER

Pooling is used for the minimization of the computing cost by reducing the dimension of the ReLU layer output. Pooling is also used to retain the position and rotational invariant features of an image. There are two types of pooling methods: Maximum and Average pooling. In maximum pooling, the maximum value of the given window is selected, while in average pooling, the average value of the window is selected . Unlike average pooling, maximum pooling suppresses the noise in the image along with feature reduction. Pooling is also used to maintain the localization of the shape of the local object in the image. The window size of 2×2 is selected for maximum pooling, which reduced the size to exactly half of the ReLU layer ($100\times75\times6$). The larger window size for the maximum pooling may result in the fine local information of the image.

The hand radiograph image obtained in this project is used five maxpooling layer. The hand radiograph image is converted to first layer 100x100x3, the second layer 50x50x9, third layer 25x25x27, fourth layer 13x13x81 and finally 13x13x243. The hand radiograph image is more accurate enhances by using five maxpooling layer. Maxpooling returns the maximum value from the portion of the image covered by the kernel. Maxpooling is done to in part to help over fitting by providing an abstracted from the representation is shown in figure 4.2.3.

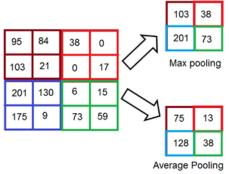


Figure 4.2.3 Max Pooling Layer

4.2.4 RESULT& DISCUSSON

The existing of the method using CNN applied in three layers. The performance of the system is evaluated based on percentage cross validation accuracy (0.6842) and loss (0.5404) is shown Table 4.2.4.1.

Table 4.2.4.1: Training of epoch for Existing system

| Training Data | Training Period | Ер | och Time |
|---------------|------------------------|----------|----------|
| (Epoch) | _ | Accuracy | Loss |
| 1/30 | 14 Seconds | 0.5263 | 0.7092 |
| 2/30 | 8 Seconds | 0.6842 | 0.6853 |
| 3/30 | 11 Seconds | 0.5000 | 0.6847 |
| 4/30 | 8 Seconds | 0.6316 | 0.6696 |
| 5/30 | 8 Seconds | 0.5526 | 0.6640 |
| 6/30 | 8 Seconds | 0.5781 | 0.7192 |
| 7/30 | 10 Seconds | 0.5625 | 0.6721 |
| 8/30 | 7 Seconds | 0.6053 | 0.6526 |
| 9/30 | 7 Seconds | 0.5526 | 0.6823 |
| 10/30 | 8 Seconds | 0.6316 | 0.6623 |
| 11/30 | 6 Seconds | 0.5526 | 0.6730 |
| 12/30 | 9 Seconds | 0.5625 | 0.6698 |
| 13/30 | 7 Seconds | 0.5938 | 0.6563 |
| 14/30 | 7 Seconds | 0.5526 | 0.6477 |
| 15/30 | 8 Seconds | 0.6053 | 0.5842 |
| 16/30 | 7 Seconds | 0.5526 | 0.7764 |
| 17/30 | 9 Seconds | 0.6579 | 0.6327 |
| 18/30 | 9 Seconds | 0.6562 | 0.5896 |
| 19/30 | 10 Seconds | 0.6579 | 0.5957 |
| 20/30 | 8 Seconds | 0.6316 | 0.5925 |
| 21/30 | 10 Seconds | 0.7368 | 0.6275 |
| 22/30 | 9 Seconds | 0.6719 | 0.6004 |
| 23/30 | 6 Seconds | 0.7500 | 0.5477 |
| 24/30 | 9 Seconds | 0.7188 | 0.5357 |
| 25/30 | 10 Seconds | 0.7188 | 0.5021 |
| 26/30 | 10 Seconds | 0.7031 | 0.5172 |
| 27/30 | 7 Seconds | 0.7368 | 0.4997 |
| 28/30 | 7 Seconds | 0.8158 | 0.3863 |
| 29/30 | 10 Seconds | 0.8158 | 0.3766 |
| 30/30 | 5 Seconds | 0.6842 | 0.5404 |

Cross Validation Accuracy = Correctly Recognition Samples * 100 / Total Number of Samples

Each epoch to gives accuracy and loss the above formula. The graph is drawn to predict the accuracy and loss of calculated epoch. Accuracy and loss is drawn based on epoch versus time duration. Accuracy graph interpreted it is positively correlated which implied if epoch increases with duration. Loss graph interpreted it is negatively correlated which stands the epoch decreases while duration increases is shown in figure 4.2.4.2.



Vol. 8, Issue 6, June 2023



Figure 4.2.4.2 Graph for Training Accuracy and Training Loss from Existing system

Five CNN layers are used in this proposed method. So that the end of my project is more accurate. The performance of the system is evaluated based on percentage cross validation accuracy (0.8947) and loss (0.4038) is shown Table 4.2.4.3

| Training Data | Training Period | Epoch Time | |
|----------------------|------------------------|------------|--------|
| (Epoch) | _ | Accuracy | Loss |
| 1/30 | 14 Seconds | 0.3684 | 0.8862 |
| 2/30 | 8 Seconds | 0.5526 | 0.6896 |
| 3/30 | 11 Seconds | 0.5781 | 0.6650 |
| 4/30 | 8 Seconds | 0.6579 | 0.7752 |
| 5/30 | 8 Seconds | 0.6316 | 0.6433 |
| 6/30 | 8 Seconds | 0.6316 | 0.6175 |
| 7/30 | 10 Seconds | 0.5938 | 0.6720 |
| 8/30 | 7 Seconds | 0.5789 | 0.6608 |
| 9/30 | 7 Seconds | 0.6316 | 0.6591 |
| 10/30 | 8 Seconds | 0.6053 | 0.6479 |
| 11/30 | 6 Seconds | 0.5789 | 0.6452 |
| 12/30 | 9 Seconds | 0.5781 | 0.6549 |
| 13/30 | 7 Seconds | 0.6053 | 0.7040 |
| 14/30 | 7 Seconds | 0.6316 | 0.6715 |
| 15/30 | 8 Seconds | 0.6053 | 0.6407 |
| 16/30 | 7 Seconds | 0.5000 | 0.6890 |
| 17/30 | 9 Seconds | 0.5938 | 0.6523 |
| 18/30 | 9 Seconds | 0.6406 | 0.6301 |
| 19/30 | 10 Seconds | 0.6094 | 0.6460 |
| 20/30 | 8 Seconds | 0.6562 | 0.5914 |
| 21/30 | 10 Seconds | 0.7188 | 0.5914 |
| 22/30 | 9 Seconds | 0.7500 | 0.5336 |
| 23/30 | 6 Seconds | 0.7632 | 0.5615 |
| 24/30 | 9 Seconds | 0.6562 | 0.6358 |
| 25/30 | 10 Seconds | 0.7812 | 0.5366 |
| 26/30 | 10 Seconds | 0.7500 | 0.5198 |
| 27/30 | 7 Seconds | 0.8158 | 0.5354 |
| 28/30 | 7 Seconds | 0.6579 | 0.5011 |
| 29/30 | 10 Seconds | 0.8438 | 0.4333 |
| 30/30 | 5 Seconds | 0.8947 | 0.4038 |

Table 4.2.4.2: Training of epoch for Proposed system

Cross Validation Accuracy = Correctly Recognition Samples * 100 / Total Number of Samples

Each epoch to gives accuracy and loss the above formula. The graph is drawn to predict the accuracy and loss of calculated epoch. Accuracy and loss is drawn based on epoch versus time duration. Accuracy graph interpreted it is positively correlated which implied if epoch increases with duration. Loss graph interpreted it is negatively correlated which stands the epoch decreases while duration increases is shown in figure 4.2.4.4,

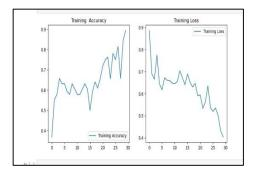


Figure 4.2.4.4 Graph for Training Accuracy and Training Loss from Proposed system

The output of the first convolution layer after the convolution of the original image of the first CNN layer resize the image to 200x200 and then passes it to ReLU layer. The 3x3 matrix is used ReLU layer (200x200x3). The max pooling layer subtracts the maximum value from the ReLU layer and converts the image to 100x100x3. The second CNN layer resize the image to 100x100x9 and then passes it to ReLU layer. The 3x3 matrix is used ReLU layer (100x100x9). The max pooling layer subtracts the maximum value from the ReLU layer and converts the image to 50x50x9. The third CNN layer resize the image to 50x50x27 and then passes it to ReLU layer. The 3x3 matrix is used ReLU layer (50x50x27). The max pooling layer subtracts the maximum value from the ReLU layer. The 3x3 matrix is used ReLU layer (50x50x27). The fourth CNN layer resize the image to 25x25x81 and then passes it to ReLU layer. The 3x3 matrix is used ReLU layer (25x25x81). The max pooling layer subtracts the maximum value from the ReLU layer and converts the image to 25x25x243 and then passes it to ReLU layer. The 6x6 matrix is used ReLU layer (25x25x243). The max pooling layer subtracts the image to 13x13x243. Finally the hand radiograph image is converted to 41067x1 in the fully connected layer. The image derived from the fully connected layer is used in the CNN classifier is shown in Table 4.2.5



| DEEP LEARNING LAYER | SUB- LAYER | FEATURE MAP SIZE |
|-----------------------|-------------------|------------------|
| CNN Layer-I | Convolution Layer | 200x200 |
| | ReLU Layer | 200x200x3 |
| | Max Pooling Layer | 100x100x3 |
| CNN LayerII | Convolution Layer | 100x100x9 |
| | ReLU Layer | 100x100x9 |
| | Max Pooling Layer | 50x50x9 |
| CNN Layer-III | Convolution Layer | 50x50x27 |
| | ReLU Layer | 50x50x27 |
| | Max Pooling Layer | 25x25x27 |
| CNN Layer-IV | Convolution Layer | 25x25x81 |
| | ReLU Layer | 25x25x81 |
| | Max Pooling Layer | 13x13x81 |
| CNN Layer-V | Convolution Layer | 25x25x243 |
| | ReLU Layer | 25x25x243 |
| | Max Pooling Layer | 13x13x243 |
| Fully Connected Layer | • | 41067x1 |

Finally the project will be detect hand print authorised person (or) unauthorised person is shown in Table 4.2.6 Table 4.2.6: Report for Pe

| S. NO. | IMAGE NUMBER | IMAGE | SIZE | RESULT |
|--------|-----------------|-------|--------|---------------------|
| 1 | 4360 | ť | 302 KB | Authorized Person |
| 2 | 4520 | ða. | 395 KB | Unauthorized Person |
| | | | | |



| | International Journal of Innovative Research in Management, Engineering, and Technology 3 4362 | | | | |
|----|--|-----|----------------------|---------------------|--|
| 3 | 4362 | | ol2\$8 K3uK & June 2 | 02Authorized Person | |
| 4 | 4521 | * | 316 KB | Unauthorized Person | |
| 5 | 4364 | -HO | 266 KB | Authorized Person | |
| 6 | 4522 | L | 327 KB | Unauthorized Person | |
| 7 | 4523 | al. | 282 KB | Unauthorized Person | |
| 8 | 4524 | 54 | 248 KB | Unauthorized Person | |
| 9 | 4368 | 8 | 372 KB | Authorized Person | |
| 10 | 4525 | - | 2,073 KB | Unauthorized Person | |
| 11 | 4370 | Y | 422 KB | Authorized Person | |



| International . | ournal of Innovative Research in Management, Engineering, and Technology |
|-----------------|--|
| | Vol. 8, Issue 6, June 2023 |

| International Journal of Innovative Research in Management, Engineering, and Technology Vol. 8, Issue 6, June 2023 | | | | |
|---|------|-----|----------|---------------------|
| 12 | 4371 | R | 1,192 KB | Authorized Person |
| 13 | 4526 | ovi | 338 KB | Unauthorized Person |
| 14 | 4527 | 4 | 242 KB | Unauthorized Person |
| 15 | 4374 | W | 303 KB | Authorized Person |
| 16 | 4528 | L: | 254 KB | Unauthorized Person |
| 17 | 4376 | | 342 KB | Authorized Person |
| 18 | 4529 | W. | 1,271 KB | Unauthorized Person |
| 19 | 4530 | 06* | 286 KB | Unauthorized Person |
| 20 | 4379 | ¥ | 3,258 KB | Authorized Person |
| | | | | |



| | International | | | ISSN (Online): 2456-0448 |
|----|---------------|---|------------------|------------------------------------|
| 21 | 4531 | | 118295uKB June 2 | ement, Engineering, and Technology |
| | | н — — — — — — — — — — — — — — — — — — — | | |
| 22 | 4532 | . * | 926 KB | Unauthorized Person |
| 23 | 4533 | 24 | 193 KB | Unauthorized Person |
| 24 | 4383 | L at | 322 KB | Authorized Person |
| 25 | 4384 | ar | 778 KB | Authorized Person |
| 26 | 4534 | E1 | 226 KB | Unauthorized Person |
| 27 | 4386 | G ^{R=1} | 215 KB | Authorized Person |
| 28 | 4387 | k. | 299 KB | Authorized Person |
| 29 | 4535 | 2 | 1,155 KB | Unauthorized Person |
| | | | | |



| International Journal of Innovative Research in Management, Engineering, and Technology 30 4536 Vol1\$9sKB6, June 2013 nauthorized Person | | | | | |
|---|------|------|--------------------|-----------------------|--|
| 30 | 4536 | Ve | 1169sKuB 6, June 2 | 13 nauthorized Person | |
| | | | | | |
| 31 | 4385 | ų, | 3,196 KB | Authorized Person | |
| 32 | 4537 | 1 | 1,313 KB | Unauthorized Person | |
| 33 | 4561 | itia | 2,132 KB | Authorized Person | |
| 34 | 4538 | Y | 1,691 KB | Unauthorized Person | |
| 35 | 4539 | 4. | 1,259 KB | Unauthorized Person | |
| 36 | 4540 | | 1,199 KB | Unauthorized Person | |
| 37 | 4563 | | 1,031 KB | Authorized Person | |
| 38 | 4541 | R. | 304 KB | Unauthorized Person | |
| | | | | | |



| 39 | International J 4565 | Journal of Innovative | e Research in Manag 118764uKB June 2 | ement, Engineering, and Technology 2Authorized Person |
|----|-------------------------|-----------------------|---|--|
| | | | | |
| 40 | 4542 | 8 | 355 KB | Unauthorized Person |
| 41 | 4543 | CK ^{ala} | 2,349 KB | Unauthorized Person |
| 42 | 4566 | ¥ | 1,127 KB | Authorized Person |
| 43 | 4544 | * | 277 KB | Unauthorized Person |
| 44 | 4545 | N. | 1,649 KB | Unauthorized Person |
| 45 | 4567 | ¥ | 876 KB | Authorized Person |
| 46 | 4546 | × | 182 KB | Unauthorized Person |
| 47 | 4388 | A. | 1,080 KB | Authorized Person |
| 48 | 4569 | | 320 KB | Authorized Person |



| | / |
|--|-----------|
| International Journal of Innovative Research in Management, Engineering, and T | Chnology |
| micinational journal of milovative Research in Management, Engineering, and 1 | Cennology |
| | <u> </u> |
| Vol. 8. Issue 6. June 2023 | |
| $v \Psi I$, o, issue 0, june 2025 | |

| International Journal of Innovative Research in Management, Engineering, and Technology Vol. 8, Issue 6, June 2023 | | | | | |
|---|------|------|-------------------------|---------------------|--|
| | | V | ψι. 0, 1880e 0, Julie 2 | | |
| 49 | 4547 | ðir. | 1,330 KB | Unauthorized Person | |
| 50 | 4548 | ¥ | 1,325 KB | Unauthorized Person | |
| 51 | 4572 | ove | 3,454 KB | Authorized Person | |
| 52 | 4549 | ¥ | 3,639 KB | Unauthorized Person | |
| 53 | 4573 | 3 | 1,763 KB | Authorized Person | |
| 54 | 4550 | | 1,066 KB | Unauthorized Person | |
| 55 | 4389 | ¢. | 175 KB | Authorized Person | |
| 56 | 4575 | R | 294 KB | Authorized Person | |
| 57 | 4551 | 41 | 254 KB | Unauthorized Person | |
| 58 | 4577 | | 570 KB | Authorized Person | |



| | Intern | ational Journal of Innovativ | ve Research in Mar | ISSN (Online): 2450-044 nagement, Engineering, and Technology | · O |
|----|--------|------------------------------|----------------------|--|------------|
| | | | /ol. 8, Issue 6, Jun | e 2023 | |
| | | -1-1 | | | |
| 59 | 4552 | ź | 288 KB | Unauthorized Person | |
| 60 | 4553 | Solution (Solution) | 3,308 KB | Unauthorized Person | |
| 61 | 4578 | W | 3,474 KB | Authorized Person | |
| 62 | 4554 | W- | 3,375 KB | Unauthorized Person | |
| 63 | 4580 | | 1,107 KB | Authorized Person | |
| 64 | 4581 | * | 170 KB | Authorized Person | |
| 65 | 4555 | W | 196 KB | Unauthorized Person | |
| 66 | 4556 | R. H | 1,224 KB | Unauthorized Person | |
| 67 | 4582 | | 239 KB | Authorized Person | |



| | | ournal of mnovauve | Research in Manag | ement, Engineering, and Technology | |
|----|------|--------------------|------------------------|------------------------------------|--|
| | | | ol. 8, Issue 6, June 2 | 023 | |
| 68 | 4557 | | 244 KB | Unauthorized Person | |
| 69 | 4585 | | 227 KB | Authorized Person | |
| 70 | 4559 | či, | 291 KB | Unauthorized Person | |

CONCLUSION AND FUTURE ENHANCEMENT

5.1 CONCLUSION

In conclusion, a novel human identification method using a deep neural network for matching hand radiographs is presented in this project. The hand radiographs are an appropriate approach for human identification. A convolutional neural network (CNN) is an artificial intelligence algorithm that presents remarkable capabilities for forensic image analysis. Recently, there has been a great deal of interest in using this technology. CNN studies show a pre-processing, feature extraction and the training of the results. The use **REFERENCES**

1)Sagar V.Joshi and Rajendra D. Kahphade, "Deep Learning Based Person AuthenticationUsing HandRadiographs: A Forensic Approach" in Proc. 2017Preparation of Papers for IEEE Access, Februarym2017 doi: 10.1109 / ACCESS.2020.2995788.

2) X. Qu, T. Wei, C. Peng and P. Du, "A Fast Face Recognition System Based on Deep Learning," in Proc. 2018 11th International Symposium on Computational Intelligence and Design (ISCID), Hangzhou, China, 2018, pp. 289-292.

3) Jie Lin, Jian-Ping Li, Hui Lin and Ji Ming, "Robust person identification with face and iris by modified PUM method," in Proc. 2009 International Conference on Apperceiving Computing and Intelligence Analysis, Chengdu, China, 2009, pp. 321-324.

4) I. Awate and B. A. Dixit, "Palm Print Based Person Identification," in Proc. 2015 International Conference on Computing Communication Control and Automation, Pune, India, 2015, pp. 781-785.

5) R. G. M. M. Jayamaha, M. R. R. Senadheera, T. N. C. Gamage, K. D. P. B. Weerasekara, G. A. Dissanayaka and G. N. Kodagoda, "VoizLock - Human Voice Authentication System using Hidden Markov Model," in Proc. 2008 4th International Conference on Information and Automation for Sustainability, Colombo, Sri Lanka, 2008, pp. 330-335.

6) S. Shunmugam and R. K. Selvakumar, "Electronic transaction authentication — A survey on multimodal biometrics," in Proc. 2014 IEEE International Conference on Computational Intelligence and Computing Research, Coimbatore, India, 2014, pp. 1-4

7) A'K. Bhat, B. Kumar and A. Acharya, "Radiographic imaging of the wrist", Indian journal of plastic surgery: official publication of the Association of Plastic Surgeons of India, vol. 44, no. 2, pp. 186-196, May 2011.

8) J. A. Kauffman, C. H. Slump, H. B. Moens, "Matching hand radiographs", in Proc. Overview of the workshops ProRISC-SAFE, November 17-18, 2005, Veldhoven, the Netherlands 2005 Nov , pp. 629-633.